

Operational Modal Analysis – Another Way of Doing Modal Testing

Mehdi Batel, Brüel & Kjær, Norcross, Georgia

Operational modal analysis (often called output-only or ambient modal analysis) is described in this article. Modal testing is performed on a plate structure with well-defined modes, resonance frequencies and damping values. Frequency Domain Decomposition (FDD) and Enhanced Frequency Domain Decomposition (EFDD) concepts are presented and applied to a plate structure. This article details the signal processing mathematical background and presents alternative curve-fitting processes.

An alternative modal analysis technique is presented in this article. A typical modal test of a structure is performed by measuring the input forces and output responses for a linear, time-invariant mechanical system. The excitation is either transient (impact hammer testing), random, burst-random or sinusoidal (shaker testing). The advanced signal processing tools used in operational modal analysis techniques allow the inherent properties of a mechanical structure (resonance frequencies, damping ratios, mode patterns) to be determined by only measuring the response of the structure without using an artificial excitation. This technique has been successfully used in civil engineering structures (buildings, bridges, platforms, towers) where the natural excitation of the wind is used to extract modal parameters.^{1, 2, 3} It is now being applied to mechanical and aerospace engineering applications (rotating machinery, on-road testing, in-flight testing).^{4,5,6}

The advantage of this technique is that a modal model can be generated while the structure is under operating conditions. That is, a model within true boundary conditions and actual force and vibration levels. Another advantage of the technique is the ability to perform modal testing in-situ, i.e., without removing parts under test. The test can be performed with other applications or activities in parallel and does not affect or interrupt daily use of the machine. The measurement technique is identical to Operational Deflection Shape (ODS) measurement procedures where one accelerometer is used as a reference and a series of accelerometers for the responses at all Degrees of Freedom (DOFs) of interest.

Figure 1 shows a schematic description of an ambient response system. The inputs to the system (that represent the excitation forces) are assumed to have a Gaussian amplitude distribution. In civil engineering applications, Gaussian excitation is typically provided by waves (offshore applications), wind or traffic load. In mechanical engineering, loads are typically generated from bearings, vibration from the road or the air, rotating components or the engine. To define all modes, the excitation should be broadband. Practically, this may involve running up an engine or modifying the frequency of excitation. In cases where the loading forces cannot be modified, the end-user needs to have at least some idea about the excitation frequencies that are generated to interpret the results and use the appropriate modal extraction method. For nonbroadband excitation, modal extraction becomes difficult and would result in poor model descriptions. The art of operational modal analysis is then to distinguish real structural behavior from noise and other measured sources.

In this study, measurements were made with a Brüel & Kjær PULSE™ Multi-Analyzer System and the Modal Test Consultant™ (Type 7753) to create the test structure geometry, assign measurement points and capture the data. The analysis was performed using the Brüel & Kjær Operational Modal Analysis™ software (Type 7760) where advanced signal processing

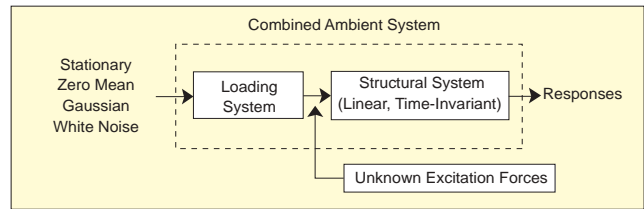


Figure 1. Combined ambient model.



Figure 2. PULSE™ multi-analysis portable system connected to test plate; hand-tapping excitation is demonstrated.

and modal extraction procedures were performed.

Measurement Procedure

The specimen used is a rectangular plate (29 cm × 25 cm) resting on a foam pad to simulate free-free boundary conditions. The measurements were made using 4 accelerometers (1 for the reference and 3 roving accelerometers for the responses at 36 DOFs). The data acquisition system was a portable PULSE™ analysis platform (see Figure 2), composed of a 4-channel portable front-end (4 inputs/2 outputs) and a laptop computer for the software.

Hand tapping the plate for each set of measurements provided enough energy to the structure. The PULSE Modal Test Consultant™ was used to set-up the hardware, create the geometry and assign the measurements to each DOF. The reference accelerometer was maintained at a well-chosen point on the plate. The reference point selection has a significant effect on measurement results. It has to be placed such that all modes contribute to the reference accelerometer. A preliminary idea of the mode shapes to be measured definitely helps in understanding where to place the reference points. Typically, points that are not nodal or peak deflection points are good choices (atypical degrees of freedom). Each data set is then composed of the reference accelerometer signal and the 3 accelerometers measuring the responses at the specified DOFs. Twelve data sets were then collected for the plate. The raw time histories were captured by a “Time Capture Analyzer” for each measurement set. A pretest measurement indicated that the lowest frequency of interest was about 350 Hz. In that case only 2 sec of data capture would be enough to represent more than 500 cycles at the lowest frequency of interest. A sample data set is shown in Figure 4. This figure also shows a Short Time Fou-

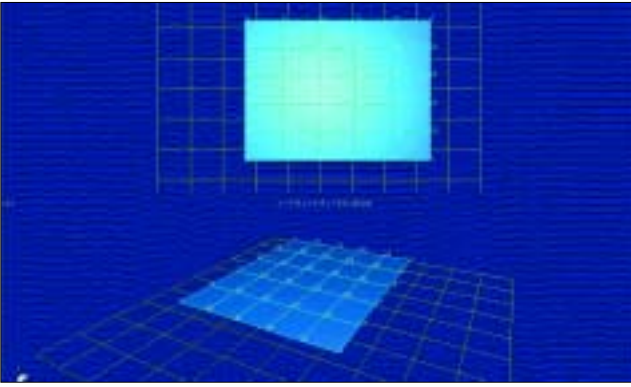


Figure 3. Two views of the plate geometry.

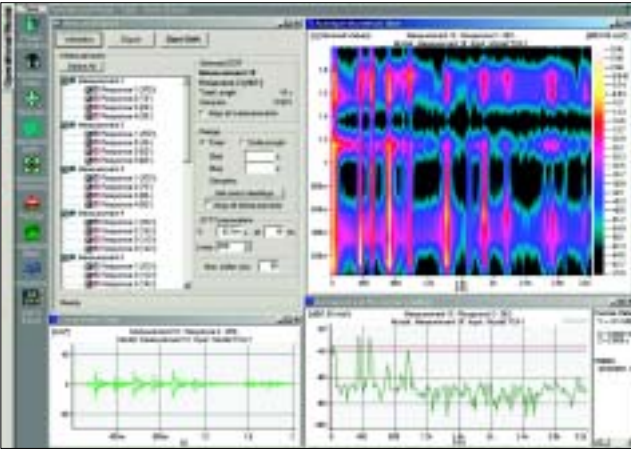


Figure 4. Sample output from the "Time Capture Analyzer" for measurement 10.

rier Transform (STFT) analysis that provides a time/frequency representation of all the responses captured.

The STFT analysis is performed by a traveling Fast Fourier Transform (FFT) window with user defined parameters. Figure 4 exhibits straight lines showing up at specific frequencies during the entire capture that correspond to structural resonances.

All the raw time data, the geometry and the series of measurements are then directly exported from the data acquisition system to the operational modal analysis curve-fitter for signal processing calculations and modal extraction.

Signal Processing and Decomposition

Preliminary Signal Processing. The first step of the analysis is to perform a Discrete Fourier Transform (DFT) on the raw time data to obtain acceleration spectral density matrices that will contain all the modal information. Since the excitation is broadband and has a continuous spectrum, the best spectral descriptor is the acceleration spectral density (g^2/Hz) that normalizes the measurements with respect to the bandwidth of the frequency analysis filter (FFT).

The analysis is performed by specifying the order of decimation (fraction of the original sampling frequency) and the number of spectral lines for the Fourier analysis. The software has the capability of applying a filter (bandpass, bandstop, highpass or lowpass) on the data to remove unwanted components that may obscure any curvefitting process in the analysis. No decimation process was chosen since an appropriate frequency range was already based on the pretest (a Nyquist frequency of 4096 Hz and a sampling frequency of 8192 Hz). The spectral estimation was performed using the modified averaged periodogram method (Welch's technique) with an overlap of 66.7% and a Hanning weighting function. This ensures that all data are equally weighted in the averaging process, minimizing leakage and picket fence effects. The Welch method performs a splitting of the time series and then an

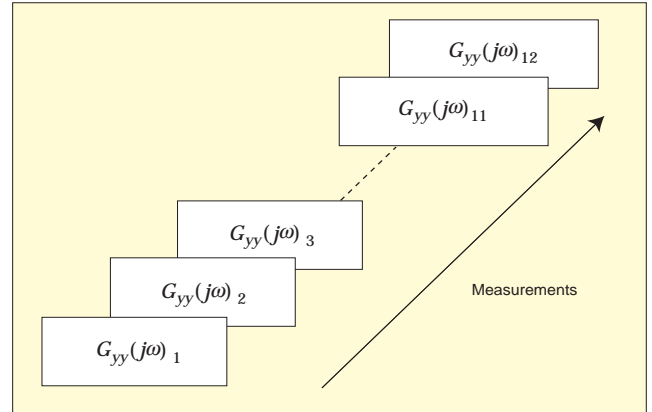


Figure 5. Cross spectral density matrix elements between the 4 responses.

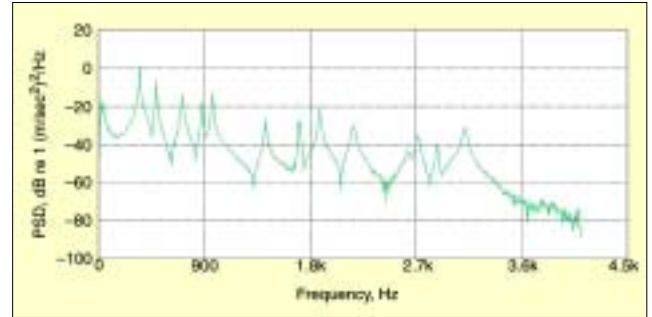


Figure 6. Magnitude of the spectral density between the reference point and response 4 for dataset 10.

overlap of the windowed segments before averaging them together. This technique minimizes spectral noise and the effects of other artifacts. Using the averaged spectrum for frequency peak-picking reduces possible misinterpretation of spectral components.

The spectral density matrices are then calculated for all the series of measurements. The size of the matrix is $n \times n$, n being the number of transducers (4 in this case, i.e., 4 measured DOFs). In this example, 12 matrices (of a size 4×4) were calculated for each frequency. Each element of those matrices is a spectral density function. The diagonal elements of the matrix are the magnitudes of the spectral densities between a response and itself (power spectral densities). The off-diagonal elements are the cross spectral densities between the 4 responses (Figure 5). All those matrices are Hermitian (symmetric with complex conjugate elements around the diagonal).

Each matrix is expressed in terms of power and cross spectral densities as follows:

$$[G_{yy}(j\omega)]_i = \begin{bmatrix} PSD_{11}(j\omega) & CSD_{12}(j\omega) & CSD_{13}(j\omega) & CSD_{14}(j\omega) \\ CSD_{21}(j\omega) & PSD_{22}(j\omega) & CSD_{23}(j\omega) & CSD_{24}(j\omega) \\ CSD_{31}(j\omega) & CSD_{32}(j\omega) & PSD_{33}(j\omega) & CSD_{34}(j\omega) \\ CSD_{41}(j\omega) & CSD_{42}(j\omega) & CSD_{43}(j\omega) & PSD_{44}(j\omega) \end{bmatrix} \quad (1)$$

$PSD(j\omega)$ denotes the power spectral density (magnitude of the auto spectral density) and $CSD(j\omega)$ denotes the cross spectral density. Since the matrices calculated are Hermitian we have

$$CSD_{pq}(j\omega) = CSD_{qp}^*(j\omega), p \neq q \quad (2)$$

The "*" symbol denotes a complex conjugate value. The $PSD_{pq}(j\omega)$ are all real valued elements, and the $CSD_{qp}(j\omega)$ take complex values, carrying the phase information between the measurement and the reference degree of freedom.

Figure 6 shows the result obtained of the spectral density calculation between response 4 and the reference accelerometer at measurement 10 (cross spectral density).

Frequency Domain Decomposition Theory Background. Frequency Domain Decomposition (FDD) is an extension of the Basic Frequency Domain (BFD) technique or more often called

the peak-picking technique. This approach uses the fact that modes can be estimated from the spectral densities calculated with the assumption of white noise input and a lightly damped structure. This nonparametric technique estimates modal parameters directly from signal processing calculations.

The FDD technique estimates the modes using a Singular Value Decomposition (SVD) of each of the spectral density matrices. This decomposition corresponds to a Single Degree of Freedom (SDOF) identification of the system for each singular value.

The relationship between the input $x(t)$ and the output $y(t)$ can be written in the following form:⁷

$$[G_{yy}(j\omega)] = [H(j\omega)]^* [G_{xx}(j\omega)] [H(j\omega)]^T \quad (3)$$

where $G_{xx}(j\omega)$ is the input power spectral density matrix that is constant in the case of a stationary zero mean white noise input. This constant will be called C in the rest of the mathematical derivation. $G_{yy}(j\omega)$ is the output PSD matrix and $H(j\omega)$ is the frequency response function (FRF) matrix. As seen in Equation (3), the output G_{yy} will be highly sensitive to the input constant C . The rest of the equation derivations and single degree of freedom identification will provide relevant results, only by assuming that the input is effectively represented by a constant value (mean Gaussian). It is therefore important to realize how this input assumption will be crucial to the technique.

The FRF matrix can be written in a typical partial fraction form (used in classical modal analysis), in terms of poles and residues

$$[H(j\omega)] = \frac{[Y(\omega)]}{[H(\omega)]} = \sum_{k=1}^m \frac{[R_k]}{j\omega - \lambda_k} + \frac{[R_k]^*}{j\omega - \lambda_k^*} \quad (4)$$

with

$$\lambda_k = -\sigma_k + j\omega_{dk} \quad (5)$$

m being the total number of modes, λ_k being the pole of the k^{th} mode, σ_k the modal damping and ω_{dk} the damped natural frequency of the k^{th} mode:

$$\omega_{dk} = \omega_{0k} \sqrt{1 - \zeta_k^2} \quad (6)$$

with

$$\zeta_k = \frac{\sigma_k}{\omega_{0k}} \quad (7)$$

ζ_k being the critical damping and ω_{0k} the undamped natural frequency, both for mode k .

$[R_k]$ is called the residue matrix and is expressed in an outer product form:

$$[R_k] = \psi_k \gamma_k^T \quad (8)$$

where ψ_k is the mode shape and γ_k is the modal participation vector. All those parameters are specified for the k^{th} mode.

The transfer function matrix $[H]$ is symmetric and an element $H_{pq}(j\omega)$ of this matrix is then written in terms of the component $r_{kpq}(j\omega)$ of the residue matrix as follows:

$$H_{pq}(j\omega) = \sum_{k=1}^m \frac{r_k(p,q)}{j\omega - \lambda_k} + \frac{r_k(p,q)^*}{j\omega - \lambda_k^*} \quad (9)$$

Using expression (3) for the matrix G_{yy} and the heaviside partial fraction theorem for polynomial expansions, we obtain the following expression for the matrix output PSD matrix G :

$$[G_{yy}(j\omega)] = \sum_{k=1}^m \frac{[A_k]}{j\omega - \lambda_k} + \frac{[A_k]^*}{j\omega - \lambda_k^*} + \frac{[B_k]}{-j\omega - \lambda_k} + \frac{[B_k]^*}{-j\omega - \lambda_k^*} \quad (10)$$

where $[A_k]$ is the k^{th} residue matrix of the matrix $[G_{yy}]$. The matrix G_{xx} is assumed to be a constant value C , since the excitation signals are assumed to be uncorrelated zero mean white noise in all the measured DOFs. This matrix is Hermitian and is described in the form:

$$[A_k] = [R_k] C \sum_{s=1}^m \frac{[R_s]^H}{-\lambda_k - \lambda_s^*} + \frac{[R_s]^T}{-\lambda_k - \lambda_s} \quad (11)$$

The contribution of the residue has the following expression:

$$[A_k] = \frac{[R_k] C [R_k]^H}{2\sigma_k} \quad (12)$$

Considering a lightly damped model, we have the following relationship:

$$\lim_{\text{damping} \rightarrow \text{light}} [A_k] = [R_k] C [R_k]^T = \psi_k \gamma_k^T C \gamma_k \psi_k^T = d_k \psi_k \psi_k^T \quad (13)$$

where d_k is a scalar constant.

The contribution of the modes at a particular frequency is limited to a finite number (usually 1 or 2). The response spectral density matrix can then be written as the following final form:

$$[G_{yy}(j\omega)] = \sum_{k \in \text{Sub}(\omega)} \frac{d_k \psi_k \psi_k^H}{j\omega - \lambda_k} + \frac{d_k^* \psi_k^* \psi_k^{*H}}{j\omega - \lambda_k^*} \quad (14)$$

where $\text{Sub}(\omega)$ is the set of modes that contribute at the particular frequency.

This final form of the matrix is then decomposed into a set of singular values and singular vectors using the Singular Value Decomposition technique (SVD). This decomposition is performed to identify single degree of freedom models of the problem.

Singular Value Decomposition. The singular value decomposition of an $m \times n$ complex matrix A is the following factorization:

$$A = U \Sigma V^H \quad (15)$$

where U and V are unitary and Σ is a diagonal matrix that contains the real singular values.

$$\Sigma = \text{diag}(s_1, \dots, s_r) \quad (16)$$

$$r = \min(m, n) \quad (17)$$

The superscript H on the matrix V denotes a Hermitian transformation (transpose and complex conjugate). In the case of real valued matrices, the V matrix is only transposed. The s_r elements in the matrix Σ are called the singular values and their following singular vectors are contained in the matrices U and V .

This singular value decomposition is performed for each of the matrices at each frequency and for each measurement (Figure 7). The spectral density matrix is then approximated to the following expression after SVD decomposition:

$$[G_{yy}(j\omega)] = [\Phi] [\Sigma] [\Phi]^H \quad (18)$$

$$\text{with } [\Phi]^H [\Phi] = [I] \quad (19)$$

Σ being the singular value matrix and Φ the singular vectors unitary matrix:

$$[\Sigma] = \text{diag}(s_1, \dots, s_r) = \begin{bmatrix} s_1 & 0 & 0 & \dots & \dots & 0 \\ 0 & s_2 & 0 & \dots & \dots & \dots \\ 0 & \dots & s_3 & \dots & \dots & \dots \\ \dots & \dots & \dots & \dots & \dots & 0 \\ \dots & \dots & \dots & \dots & s_r & 0 \\ 0 & \dots & \dots & 0 & 0 & 0 \end{bmatrix} \quad (20)$$

$$[\Phi] = \{[\phi_1] \{ \phi_2 \} \{ \phi_3 \} \dots \{ \phi_r \} \} \quad (21)$$

The number of nonzero elements in the diagonal of the singular matrix corresponds to the rank of each spectral density matrix. The singular vectors correspond to an estimation of the mode shapes and the corresponding singular values are the spectral densities of the SDOF system expressed in Equation (14).

Figure 8 shows the result of the singular value decomposition of the spectral density matrix at measurement 10. We obtain 4 singular values and 4 singular vectors for each of the spectral density matrices. The singular values and their corresponding singular vectors are ranked in singular value de-

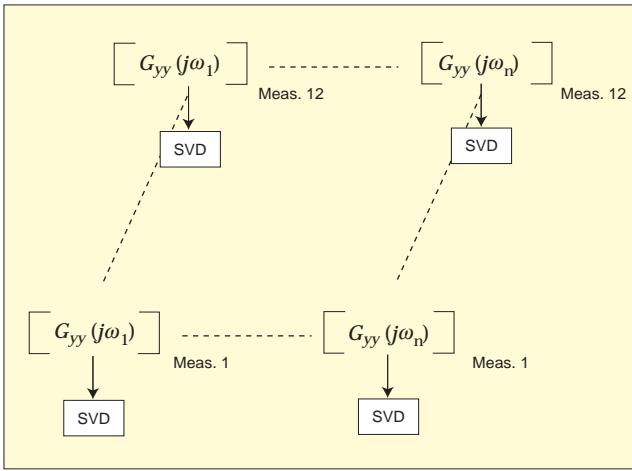


Figure 7. Singular value decomposition procedure for the spectral density matrix at each frequency.

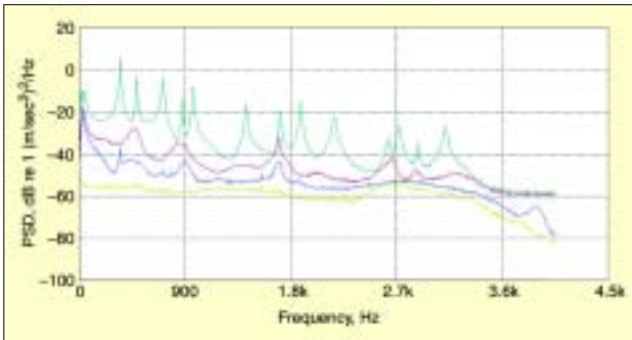


Figure 8. Result of the SVD for measurement 10.

scending order for each of the spectral density matrices, meaning that the first singular value will be the largest.

The green curve shows the first singular value and the other curves show the 3 remaining singular values. There are as many singular values as measured DOFs (4 in this case) for a particular measurement (measurement 10 in the figure). This technique allows us to identify possible coupled modes that are often indiscernible as they appear on the spectral density functions. If only one mode is dominating at a particular frequency, then only one singular value will be dominating at this frequency. In the case of close or repeated modes, there will be as many dominating singular values as there are close or repeated modes.

Frequency Domain Decomposition – Peak-Picking and Mode Determination. Each of the SDOF systems obtained by the singular value decomposition allows us to identify the natural frequency and mode shape (unscaled) at a particular peak. Using the operational modal analysis software, we perform the peak-picking technique (similar to the quadrature-picking in classical modal analysis) for each resonance on the average of the normalized singular values for all data sets (see Figure 9). The FDD technique provided the resonance frequencies and the mode shapes listed in Table 1. The very well defined deformation patterns were animated using the software and exhibit very clear modal deformations (Figure 10).

The frequency domain decomposition provided very good results for the resonance frequencies and the mode shapes. It

Table 1. First six plate modes.

Mode	Resonance Frequency
1 – Torsional (1,1)	352.0 Hz – FDD
2 – Flexural (2,0)	492.0 Hz – FDD
3 – Flexural (0,2)	716.0 Hz – FDD
4 – Torsional (2,1)	868.0 Hz – FDD
5 – Torsional (1,2)	972.0 Hz – FDD
6 – Flexural (3,0)	1424.0 Hz – FDD

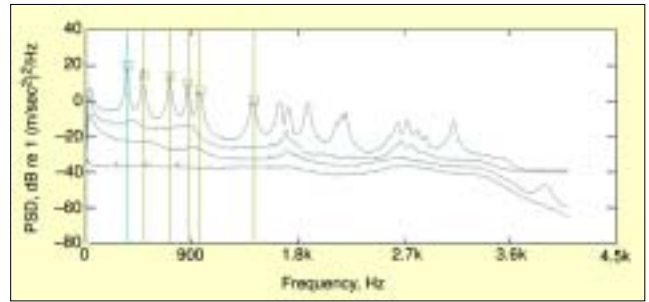


Figure 9. Peak-picking of the average normalized singular values of the complete PSD matrix.

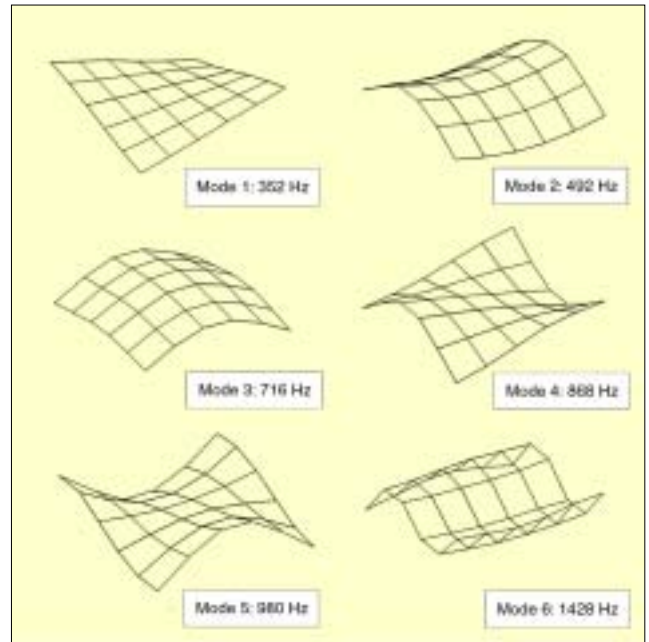


Figure 10. Three dimensional renderings of plate deformation patterns.

is important to note that the deformations obtained are not true mode shapes. The residues obtained in the mathematical derivation are not scaled to the input force and therefore will not provide scaled shape vectors.

It is also possible to obtain damping characteristics of each mode and more precise resonance frequencies by using the enhanced frequency domain decomposition based on the determination of the correlation functions.

Enhanced Frequency Domain Decomposition (EFDD). The enhanced FDD technique allows the resonance frequency and damping of a particular mode to be extracted by computing the auto- and cross-correlation functions. The SDOF power spectral density function identified around a resonance peak is returned to the time domain using the Inverse Discrete Fourier Transform (IDFT). The resonance frequency is obtained by determining zero crossing times and damping by the logarithmic decrement of the corresponding SDOF normalized auto correlation function.

The free-decay time domain function (the correlation function of the SDOF system) is used to estimate damping for mode k :

$$\delta_k = \frac{2}{P} \ln \left(\frac{r_{0k}}{|r_{pk}|} \right) \quad (22)$$

where r_{0k} is the initial value of the correlation function and r_{pk} is the p^{th} extrema. The critical damping ratio for mode k is obtained with the formula:

$$\zeta_k = \frac{\delta_k}{\sqrt{\zeta_k^2 + 4\pi^2}} \quad (23)$$

The damped natural frequency is obtained by linear regression of the crossing times corresponding to the extrema of the cor-

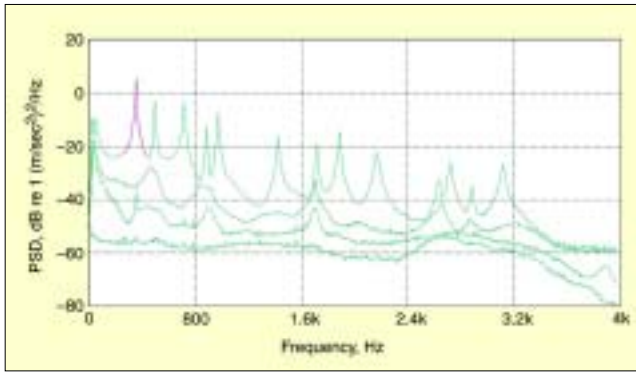


Figure 11. Singular value spectral bell identification for measurement 10.

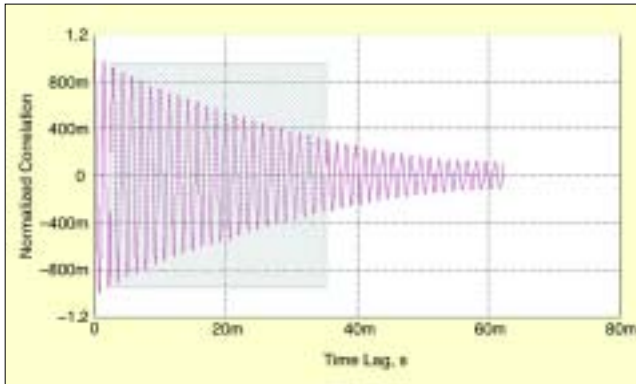


Figure 12. Normalized correlation function for measurement 10.

relation function. The undamped natural frequency for mode k is then:

$$f_{0k} = \frac{f_{dk}}{\sqrt{1 - \xi_k^2}} \quad (24)$$

Both parameters and an improved version of the mode shapes are estimated from the *SDOF Bell functions*. The SDOF Bell function is estimated using the mode determined by the previous FDD peak-picking operation. The latter is used as a reference vector in a correlation analysis based on the Modal Assurance Criteria (MAC). A MAC value is computed between the reference FDD vector and a singular vector for a particular frequency region. The MAC value describes the degree of correlation between 2 modes (it takes a value between 0 and 1) and is defined as follows for 2 vectors Φ and Ψ :

$$\text{MAC}(\{\Phi\}, \{\Psi\}) = \frac{\|\{\Phi\}^* \{\Psi\}\|^2}{\|\{\Phi\}\| \|\{\Psi\}\|} \quad (25)$$

If the largest MAC value of this vector is above a user-specified *MAC Rejection Level*, the corresponding singular value is included in the description of the SDOF Spectral Bell function. The lower this MAC Rejection Level the larger the number of singular values included in the identification of the SDOF Bell function. A good compromise value for this rejection criteria is 0.9. An average value of the singular vector (weighted by the singular values) is then obtained.

Figure 11 shows the estimated SDOF Bell function with a MAC rejection level of 0.9. The value of the MAC rejection criteria has to be chosen so that we obtain a good representation of the Bell function around the peak chosen and not include any noise around it. Noise is often present in an ambient modal analysis.

Using this SDOF Bell function, we perform an inverse Fourier transform for the determination of damping and natural frequency. The obtained normalized correlation function is shown in Figure 12.

Figure 12 exhibits a typical response of a resonating system that decays exponentially. The scattered region indicates the part of the correlation function that is used for the estimation



Figure 13. Damping ratio estimation from the decay curve of the correlation function.

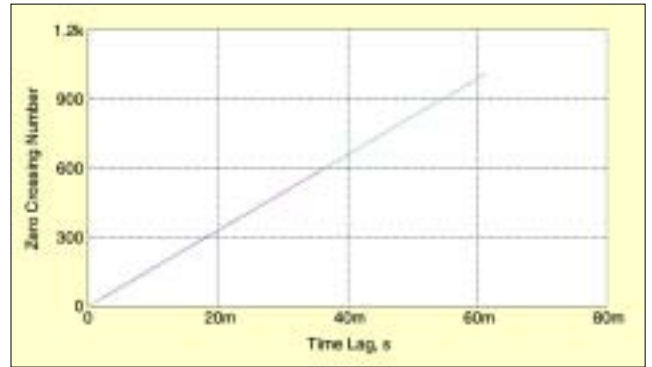


Figure 14. Natural frequency estimation.

algorithm. In that example, the modes are well spaced in the frequency domain and will provide leakage-free correlation functions. In cases where frequency peaks are not clearly spaced, leakage will definitely affect the Inverse Fourier process since only a limited frequency range is used for the Fourier calculations.

Damping is estimated by the logarithmic decrement technique of Equation 22 and the logarithmic envelope of the correlation function. The estimation is performed with a linear regression technique (red part of the curve in Figure 13). The resonance frequency is simply obtained by counting the number of times the correlation function crosses the zero axis (see Figure 14). This gives more accurate results than the simple FFD peak picking method.

The result of the regression is shown as a red line. It is important to note that the Bell functions and the estimation of the damping and natural frequency is performed for each set of measurements. The result is then obtained by averaging all the data sets together. Both the average value and the standard deviation of damping and natural frequency are calculated from the data sets.

Validation between FDD and EFDD Technique. Table 2 presents a comparison between the two techniques for the determination of resonance frequencies. It also presents the damping ratios calculated for each mode in the case of the EFDD analysis. The Mode shapes are also compared using the software and a MAC value is presented in the MAC matrix shown in Figure 15. The MAC values are very close to 1 for all modes

Table 2. Comparison of FDD and EFDD techniques for determining resonance frequencies.

Mode	FDD (Hz)		EFDD	
	FDD (Hz)	EFDD (Hz)	Damping (%)	MAC
(1,1)	352	373.34	0.75	0.988
(2,0)	492	486.80	0.64	0.986
(0,2)	716	712.10	0.41	0.998
(2,1)	868	857.53	0.48	0.968
(1,2)	972	969.68	0.48	0.996
(3,0)	1424	1418.88	0.48	0.996

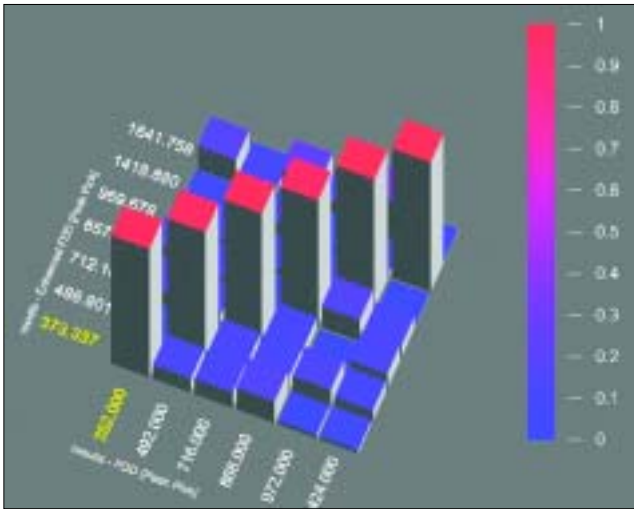


Figure 15. Mode shape comparison – MAC values.

revealing a strong correlation between the two modal extraction techniques.

Further Investigations: SSI Parametric Technique. The FDD and EFDD techniques can be correlated with a parametric technique called the Stochastic Subspace Identification (SSI) technique.^{8,9,10} This technique has been widely used in the domain of structural mechanics and allows the user to compare results obtained from both signal processing calculations and time-domain model parameterizations. The SSI technique involves the use of statistics, optimal prediction, linear system theory and stochastic processes. A brief description of the principles of this technique will be made here.

The dynamic system is expressed in terms of inertial (mass), dissipative (damping) and restoring (stiffness) matrices. It is written in terms of a linear set of differential equations of the type:

$$[M]\{\ddot{x}(t)\} + [C]\{\dot{x}(t)\} + [K]\{x(t)\} = \{f(t)\} \quad (26)$$

By rewriting the equations of motion in a classical state-space formulation often used in modern control theory, the dynamic system is expressed as follows:

$$\begin{cases} \dot{x}_t = [A]x_t + w_t \\ y_t = [C]x_t + v_t \end{cases} \quad (27)$$

where x_t represents the Kalman sequences found by an orthogonal-projection technique. The first equation (state equation) represents the dynamic behavior of the physical system and the second equation (observation equation) is called the output equation. The measured response y_t is generated by 2 stochastic processes w_t and v_t that represent the unmeasured and unknown noise processes. The matrix A is called the state matrix and the matrix C is called the observation matrix.

This technique uses a mathematical framework based on stochastic processes. A stochastic process is a mathematical modelization of a physical phenomenon that is not deterministic and is somehow not predictable from the knowledge of the present state of the system.

The intrinsic randomness of the operational modal analysis technique makes stochastic techniques very suitable for modeling a physical system. The SSI technique works on the raw time data and tries to fit a model to the data captured from the responses at the degrees of freedom.

The system represented in Equation (27) can be rewritten in the following form:

$$\begin{cases} \hat{x}_{t+1} = [A]\hat{x}_t + [K]e_t \\ y_t = [C]\hat{x}_t + e_t \end{cases} \quad (28)$$

The matrix K is the non-steady state Kalman gain (covariance matrix), and e_t is the innovation Gaussian process. X_t and x_{t+1} are the corresponding prediction state vectors for Equation (27).

The idea behind the SSI technique is to be able to represent the system in Equation (28) in the frequency domain in terms of a Transfer Function that involves the matrices A , C , K , and the identity matrix. The eigenvalue decomposition of the matrix A leads to a representation of the transfer function matrix that contains the modal parameters (natural frequencies and damping ratios). The mode shapes are extracted from the eigenvectors of the matrix A and the observation matrix C .

This technique can be used to compare and validate the results obtained by the nonparametric techniques (FDD and EFDD). It is possible to calculate the MAC and confidence factor values for 2 modes calculated by the two techniques. Furthermore, this comparison can be used to detect and differentiate the actual structural resonances and the harmonic components that often appear in rotating machinery analysis. Comparing this technique with the nonparametric methods is also very useful to determine the modes that actually correspond to a physical solution of the problem related to a logical motion of the structure. Indeed the peak-picking technique assumes that the peak detected and extracted is due to a modal structural motion and not to excessively high operation forces.

Conclusions

The operational modal analysis technique allows a scientist, technician or engineer to perform a modal investigation easily, quickly and accurately. It can be accomplished by only measuring the response of the structure subjected to unknown and unmeasured input forces (still assumed to be broadband and stationary).

It is very important to realize that this technique provides operating deformation patterns and not scaled mode shapes (no identification of modal masses). Modal analyses performed with known excitations will provide modes that are scaled to the input force and therefore can be utilized for other techniques like structural dynamics modifications or frequency response simulations. In order to obtain a full description of all relative modal parameters, it is important to note that known energy force levels (provided by a force transducer and a well-defined excitation) have to be determined, regardless of the sophistication of signal processing techniques. Impact or shaker testing are still excellent ways to perform modal testing and remain the only modal techniques that will provide scaled mode shapes and modal masses for simulation purposes.

References

1. Brincker, R., Zhang, L., and Andersen, P., "Modal Identification from Ambient Response Using Frequency Domain Decomposition," Proc. of the 18th International Modal Analysis Conference, San Antonio, TX, February 7-10, 2000.
2. Schwarz, Brian, and Richardson, M. H., "Modal Parameter Estimation from Ambient Response Data," presented at IMAC 2001, February 5-8, 2001.
3. Schwarz, Brian, and Richardson, M. H., "Post-Processing Ambient and Forced Response Bridge Data To Obtain Modal Parameters," Proceedings of the IMAC XIX Conference, Orlando, FL, Feb. 5-8, 2001.
4. Herlufsen, H., and Møller, N., "Operational Modal Analysis of a Wind Turbine Wing Using Acoustical Excitation," Brüel & Kjær Application Note, 2002.
5. Møller, N., Brincker, R., Herlufsen, H., Andersen, P., "Modal Testing of Mechanical Structures Subject to Operational Forces," IMAC XIX.
6. Brincker, R., Andersen, P., and Møller, N., "Output-Only Modal Testing of a Car Body Subject to Engine Excitation," Proc. of the 18th International Modal Analysis Conference, San Antonio, TX, February 7-10, 2000.
7. Bendat, Julius S., and Piersol, Allan G., *Random Data, Analysis and Measurement Procedures*, John Wiley and Sons, 1986.
8. Brincker, R., and Andersen, P., "ARMA (Auto Regressive Moving Average) Models in Modal Space," Proc. of the 17th International Modal Analysis Conference, Kissimmee, FL, 1999.
9. Peeters, Bart, and DeRoeck, Guido, "Reference-Based Stochastic Subspace Identification for Output-Only Modal Analysis," *Mechanical Systems and Signal Processing*, July 1999.
10. Van Overschee, P., and DeMoor, B., *Subspace Identification for Linear Systems*, Kluwer Academic Publishers, 1996. 

The author can be contacted at: mehdi.batel@bksv.com.